COOLING EFFECTIVENESS OF MIST PRECOOLER FOR IMPROVING ENERGY PERFORMANCE OF AIR-COOLED CHILLER

by

Fu Wing YU[a,*], Kwok Tai CHAN[b], Jia YANG[b], and Rachel Kam Yung SIT[a]

[a] Hong Kong Community College, The Hong Kong Polytechnic University, Hong Kong
[b] Department of Building Services Engineering, The Hong Kong Polytechnic University, Hong Kong

Original scientific paper
https://doi.org/10.2298/TSCI151112071Y

Mist is increasingly applied to precool outdoor air in heat rejection. This study investigates how the coefficient of performance of an air-cooled chiller varies with a mist precooler at different levels of cooling effectiveness. A multi-variate regression model was developed to simulate the operating variables of an air-cooled chiller with mist precooling. The model was validated with typical performance data of an air-cooled centrifugal chiller. The coefficient of performance would increase by up to 30%, depending on the cooling effectiveness and the wet bulb depression – the difference between the dry bulb and wet bulb temperatures of outdoor air. At a large wet bulb depression, the percentage increase of coefficient of performance tended to correlate linearly with the chiller capacity. Yet at a small wet bulb depression, the dynamic control of condensing temperature resulted in a non-linear relationship between the percentage change of coefficient of performance and the cooling effectiveness. Further experimental work is required to optimize cooling effectiveness for the maximum coefficient of performance.

Key words: *air-cooled chiller, coefficient of performance, mist precooling*

Introduction

The energy performance of vapour compression refrigeration systems is strongly influenced by heat rejection methods. Considering water as a scarce source, heat rejection by outdoor air is an evitable choice. For an air-cooled chiller providing a given cooling capacity, the range of dry bulb temperatures of outdoor air dictates the compressor power required. This is because the condensing temperature is designed to hover above the dry bulb temperature by 10-20 °C, depending on the heat rejection capacity of condensers and the operation of condenser fans. Precooling of outdoor air is a viable means to lower the condensing temperature and, in turn, enhance the energy performance of refrigeration systems with heat rejection by outdoor air. Using a limited amount of water in the form of mist, the dry bulb temperature of the unsaturated outdoor air can drop down to the wet bulb temperature following an adiabatic (roughly constant enthalpy) process. As no cooling energy is required, this kind of evaporative cooling is widely used to reduce the electricity taken by conventional air-conditioning systems in hot-humid regions [1]. Evaporative cooling of outdoor air is increasingly applied to enhance heat rejection in refrigeration systems and hence to improve their energy performance, as mentioned in [2-7]. Direct evaporative coolers and mist precoolers are devices which can be retro-

* Corresponding author, e-mail: ccyufw@hkcc-polyu.edu.hk

fitted to existing air-cooled chiller systems to precool outdoor air and hence to enhance their energy performance [8, 9]. To familiarize with the actual installation of a direct evaporative cooler and a mist precooler, please refer to [10] and fig. 2 in [11]. Mist precoolers are preferable than direct evaporative coolers, considering the ease of installation and the negligible air-flow resistance [9]. At present, there is no standard design for such evaporative cooling devices and no standard protocol to verify their cooling effectiveness.

The benefits of mist precooling for air-cooled chillers have been identified from a series of experimental and simulation studies [10-15]. When the outdoor air was cooled by mist to its saturation state, the coefficient of performance (*COP*) increased to 21.3%, when the chiller operated under head pressure control (HPC) with a high condensing temperature in all outdoor conditions. If the condensing temperature were under optimal control with precooled outdoor air, the *COP* would further rise by up to 51.5%. This *COP* increase brought a 14.1% decrease in the annual electricity consumption of a chiller system operating under a subtropical climate [12]. Another reduction of 19.8% in the annual electricity consumption was identified when the chiller system had five identical chillers operating under floating condensing temperature control (FCTC) with an optimum mist generation rate [15]. The FCTC means the condensing temperature can float freely within its boundary to minimize the sum of compressor power and condenser fan power for a given operating condition. Regardless of the setting of condensing temperature, the mist precooling enabled the annual electricity consumption to drop by 8.1-9.9% when the chiller system operated under the typical and future climate scenarios of Hong Kong [13].

The extent to which the dry bulb temperature can drop is governed by cooling effectiveness $\eta_{ce} = (T_{db} - T'_{db})/(T_{db} - T_{wb})$. The difference $(T_{db} - T_{wb})$ is called the wet bulb depression. The cooling effectiveness of mist precoolers varies from 0 to 1 and if T'_{db} drops to T_{wb} – the lower boundary, T_{wb}, then η_{ce} is equal to 1. The cooling effectiveness of mist precoolers depends on two factors. The first is how nozzles are located to distribute an adequate amount of mist in front of the condensers. The second is how the mist can be fully evaporated when entraining the condenser air stream with different flow rates based on the operating conditions of air-cooled chillers.

Several studies have discussed the parameters interacting η_{ce} when applying mist precooling to air-cooled chillers. According to experimental work by Yang *et al.* [12], η_{ce} varied from 0.30 to 0.91 for a fixed mist generation rate and a small wet bulb depression caused a low η_{ce}. The highest level of η_{ce} was dictated by the mist generation rate to meet the designed heat rejection air-flow and the designed temperature conditions of outdoor air. Tissot *et al.* [16] investigated how the *COP* and refrigeration effect of an air conditioner varied with different mist generation rates at different combinations of dry bulb temperature and relative humidity. At a low relative humidity, a high mist generation rate could further improve the refrigeration effect and *COP*. As the face area of an air-cooled condenser is large, an even distribution of mist over the whole area is required to ensure the uniform and high η_{ce}. Tissot *et al.* [17] addressed this issue in their numerical analysis on mist evaporation in the upstream flow of condenser air. The size and injection direction of mist interacted η_{ce} in a complex manner. Mist droplets with a size of greater than 25 μm in diameter could spread effectively over a wide area while very small mist droplets tended to concentrate together with low dispersion ability. The cooling effectiveness of mist precoolers would be enhanced with a higher evaporation effect when the mist droplets and air stream were in the counter-flow direction. The interaction between η_{ce} and the droplet size would be more complicated when the flow rate of condenser air varied with the control of condenser fans.

It is expected that the interaction between the operating variables of a chiller and a mist precooler poses a challenge in maximizing their performance within their operating boundaries. This study investigates the change of chiller *COP* at different levels of η_{ce}. A multivariate regression model has been developed to simulate the operating variables of an air-cooled centrifugal chiller with a mist precooler. Physical parameters and performance data used to validate the model will be presented. A parametric study will be carried out on how a chiller *COP* varies with η_{ce} at different load and climatic conditions. The relationship between the operating variables of the chiller and the mist precooler will be discussed. The significance of the study is to provide insights on what parameters influence the design and operation of mist precoolers to achieve the maximum η_{ce}. The improved chiller *COP* at part load operation would facilitate the optimization of chiller sequence control in a multiple-chiller system [18].

Description of the chiller and its model

The chiller had a nominal capacity of 1266 kW with a *COP* of 3.19 at an entering condensing air temperature of 35 °C. It was equipped with a flooded type evaporator, an air-cooled condenser, an orifice as an expansion valve, and a centrifugal compressor with capacity modulation by inlet guide vanes. Chilled water was circulated to the evaporator at a nominal flow rate of 54 L per second based on a temperature difference of 5.6 °C at the full load condition. The temperature difference of chilled water dropped from 5.6 °C when the cooling capacity reduced from 1266 kW. The condenser contained three identical fans delivering a total heat rejection air-flow rate of 118 m^3/s at full speed. Each condenser fan had a rated power of 10 kW. Table 1 summarizes the performance data collected from a chiller manufacturer when the chiller operated under HPC. The data were measured under standard rating conditions in AHRI standard 550/590 [19].

Table 1. Performance data of the chiller under HPC

Percent load [%]	Entering condenser air temperature, [°C]											
	10		15		20		25		30		35	
	COP	T_{cd}	*COP*	T_{cd}	*COP*	T_{cd}	*COP*	T_{cd}	*COP*	T_{cd}	*COP*	T_{cd}
25	1.88	45.4	1.87	45.5	1.86	45.6	1.85	45.8	1.83	46.1	1.81	46.4
50	3.06	45.9	3.04	46.0	3.02	46.2	3.00	46.5	2.97	46.7	2.94	47.1
75	3.59	46.5	3.57	46.7	3.54	46.9	3.51	47.2	3.48	47.5	3.45	47.8
100	3.49	47.3	3.47	47.5	3.44	47.8	3.41	48.1	3.38	48.3	3.19	50.4

A series of eqs. (1)-(15) were used to model the chiller. Figure 1 shows the chiller components with the corresponding modelling equations. The modelling approach is based on the regression-based chiller models used in EnergyPlus [20] but modifications were made to enhance the capability of simulating an adjustable condensing temperature and mist precooling at different levels of η_{ec}. EnergyPlus [20] is widely used to perform building system simulation and analysis. The modelling approach is sophisticated enough to carry out energy analysis of chiller systems under the steady-state condition, given an hour-by-hour building cooling load profile. The modified chiller model in this analysis can be used to perform an hour-by-hour simulation of electricity consumption of a chiller system based on a given building cooling

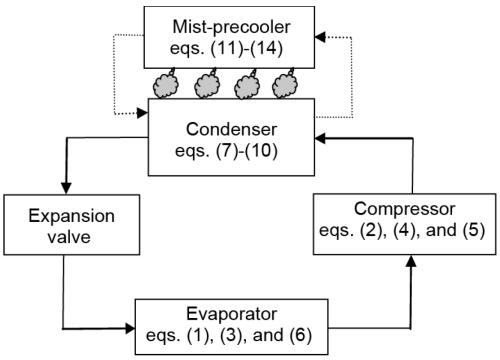

Figure 1. Chiller components and modelling equations

load profile and hourly weather data of a given city.

Under the vapour compression cycle, the variation of saturated evaporating temperature and saturated condensing temperature depends on the T_{chws} and T_{cdae}, respectively. The T_{chws} and T_{cdae} were, therefore, used to adjust chiller capacity and compressor efficiency at full load condition, as shown in eqs. (1) and (2). Equation (4) was modified to adjust compressor efficiency at part load operation when the T_{cd} was controlled at different set points. Equations (6)-(9) are related to fundamental thermal energy equations for calculating the chiller capacity output, heat rejection, and heat rejection air-flow rate.

$$CAPFT = a_0 + a_1(1.8T_{chws} + 32) + a_2(1.8T_{chws} + 32)^2 + a_3(1.8T_{cdae} + 32) + \\ + a_4(1.8T_{cdae} + 32)^2 + a_5(1.8T_{chws} + 32)(1.8T_{cdae} + 32) \quad (1)$$

$$EIRFT = b_0 + b_1(1.8T_{chws} + 32) + b_2\,(1.8T_{chws} + 32)^2 + b_3(1.8T_{cdae} + 32) + \\ + b_4\,(1.8T_{cdae} + 32)^2 + b_5(1.8T_{chws} + 32)(1.8T_{cdae} + 32) \quad (2)$$

$$PLR = \frac{Q_{cl}}{Q_{cl,\text{rated}} CAPFT} \quad (3)$$

$$EIRFPLR = c_0 + c_1 PLR + c_2 PLR^2 + c_3 T_{cd} + c_4 T_{cd}^2 + c_5 PLR\, T_{cd} \quad (4)$$

$$P_{cc} = P_{cc,\text{rated}}\, CAPFT\, EIRFT\, EIRFPLR \quad (5)$$

$$Q_{cl} = m_w\, c_{pw}\, (T_{chwr} - T_{chws}) \quad (6)$$

$$Q_{cd} = Q_{cl} + E_{cc} \quad (7)$$

$$V_a = \frac{Q_{cd}}{\rho_a c_{pa} Eff_{cd} (T_{cd} - T_{cdae})} \quad (8)$$

$$Eff_{cd} = \frac{T_{cdal} - T_{cdae}}{T_{cd} - T_{cdae}} \quad (9)$$

$$P_{cf} = P_{cf,\text{rated}} \frac{V_a}{V_{a,\text{rated}}} \quad (10)$$

$$\eta_{ce} = \frac{T_{db} - T'_{db}}{T_{db} - T_{wb}} \quad (11)$$

$$T'_{db} = \frac{H_{db} - 2501 W'_{db}}{1.006 + 1.805 W'_{db}} \quad (12)$$

$$W'_{\mathrm{db}} = W_{\mathrm{db}} + \frac{m_{\mathrm{mist}}}{V_{\mathrm{a}}\rho_{\mathrm{a}}} \tag{13}$$

$$P_{\mathrm{mp}} = 22.5 m_{\mathrm{mist}} \tag{14}$$

Equations (11)-(14) were used to simulate the evaporative cooling of mist. The constant proportion of of 22.5 kW per kg/s in eq. (14) is associated with a situation where the pump power rated at 4.5 kW drops linearly with the peak mist generation rate at 0.2 kg/s. The rated power of the mist generation pump accounts for 15% of the rated power of 30 kW in the total condenser fans. The overall *COP* is given by eq. (15):

$$COP = \frac{Q_{\mathrm{cl}}}{P_{\mathrm{cc}} + P_{\mathrm{cf}} + P_{\mathrm{mp}}} \tag{15}$$

Table 2 summarizes the physical parameters of the chiller at the full load condition based on physical data of the chiller and the equation coefficients a_{i}, b_{i}, and c_{i} determined from model validation based on performance data by the chiller manufacturer.

Table 2. Parameters and coefficients for modelling the chiller

Equation coefficients
CAPFT: $a_0 = -0.09464899$; $a_1 = 0.0383407$; $a_2 = -0.00009205$; $a_3 = 0.00378007$; $a_4 = -0.00001375$; $a_5 = -0.00015464$
EIRFT: $b_0 = 0.13545636$; $b_1 = 0.02292946$; $b_2 = -0.00016107$; $b_3 = -0.00235396$; $b_4 = 0.00012991$; $b_5 = -0.00018685$
EIRFPLR: $c_0 = 0.26558046$; $c_1 = 0.42690172$; $c_2 = 1.01894459$; $c_3 = -0.00830353$; $c_4 = 0.00029512$; $c_5 = -0.02176401$
Parameters
$Q_{\mathrm{cl,rated}} = 1266$ kW, $P_{\mathrm{cc,rated}} = 428$ kW, $V_{\mathrm{a,rated}} = 118$ m^3/s, $P_{\mathrm{cf,rated}} = 30$ kW

Figure 2 shows the procedure to solve the operating variables in the equations. The T_{chws} is maintained at 7 °C for all operating conditions. An initial condensing temperature T_{cd0} of 50 °C was used at the beginning of each iteration. To validate the model, combinations of Q_{cl} at 317, 633, 950, 1266 kW, and T_{db} at 10, 15, 20, 25, 30, and 35 °C given in tab. 1 were the input data. This constituted 24 sets of operating conditions. In the absence of mist precooling, dummy values for *RH* and η_{ce} were 100% and 0, respectively.

Table 3 shows the values assigned to the input variables to carry out the parametric analysis with the validated model. The range of Q_{cl} is from half to full capacity, as chillers often operate at above 50% capacity in a multiple-chiller system

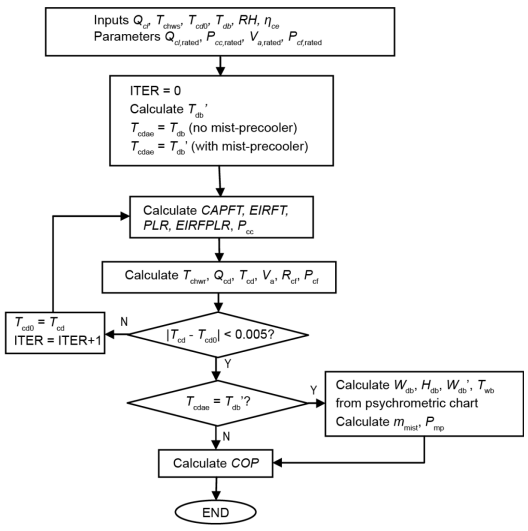

Figure 2. Procedure to evaluate operating variables of the chiller

with sequencing control. Sequencing control means that one more chiller is staged when all the chillers are operating at above their full capacity. The ranges of T_{db} and RH are related to typical climatic conditions for chillers operating in sub-tropical regions. Mist evaporation at RH of above 85% has no apparent effect on cooling as the wet bulb depression is small. A full range for η_{ce} from 0 to 1 was considered. Based on the flowchart in fig. 2, T_{cd0} was fixed under HPC. To perform FCTC, T_{cd} was decreased by 0.05 °C in each iteration successively until the sum of P_{cc} and P_{cf} was minimized.

Table 3. Values for the input variables in parametric analysis

Input variable	Values assigned
Q_{cl} [kW] (% full load)	633 (50%), 760 (60%), 886 (70%), 1013 (80%), 1139 (90%), 1266 (100%)
T_{db} [°C]	15, 20, 25, 30, 35
RH [%]	40, 50, 60, 70, 80, 85
η_{ce}	0, 0.2, 0.4, 0.6, 0.8, 1

Results and discussion

Model validation

Figure 3 shows a scatter plot of the modelled *COP* against the actual *COP*. The R^2 of the modelled *COP* from the actual *COP* is 0.9638. This means that 96.38% of the variation of the actual *COP* can be explained by the corresponding variation of the modelled *COP* using their linear regression relationship.

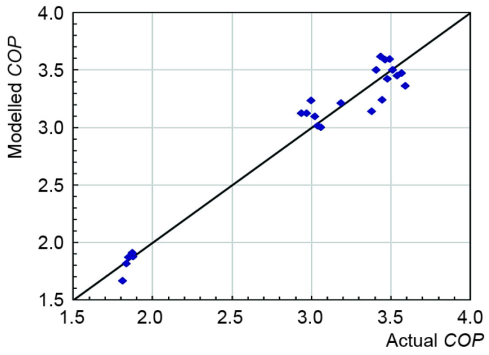

Figure 3. Scatter plot of the modelled *COP* against the actual *COP*

Parametric analysis of COP at different levels of cooling effectiveness

Any given dry bulb temperature with lower relative humidity gives a higher wet bulb depression. This results in a greater drop in the dry bulb temperature at a given cooling effectiveness. Figures 4 to 7 show how the percentage change of *COP* varies at different percentages of chiller capacity and different levels of cooling effectiveness when the chiller operated under HPC and FCTC. Compared fig. 4 with fig. 5, and fig. 6 with fig. 7, the percentage increase of *COP* is more significant under FCTC than that under HPC. This indicates that mist precooling complements FCTC to further improve the *COP*. At the low relative humidity of 40% with a high wet bulb depression, the percentage increase of *COP* appears to rise linearly with the chiller capacity. This favours the multiple-chiller arrangement in which the chillers tend to operate near full capacity for most operating hours. The percentage change of *COP* increases with the cooling effectiveness for any given chiller capacity. The highest percentage increase of about 30% can be achieved at the highest dry bulb temperature of 35 °C with a 9 °C wet bulb depression when the cooling effectiveness is one.

As fig. 6 illustrates, at a high relative humidity of 85% with a low wet bulb depression, the percentage increase of *COP* becomes small and appears to keep constant at different

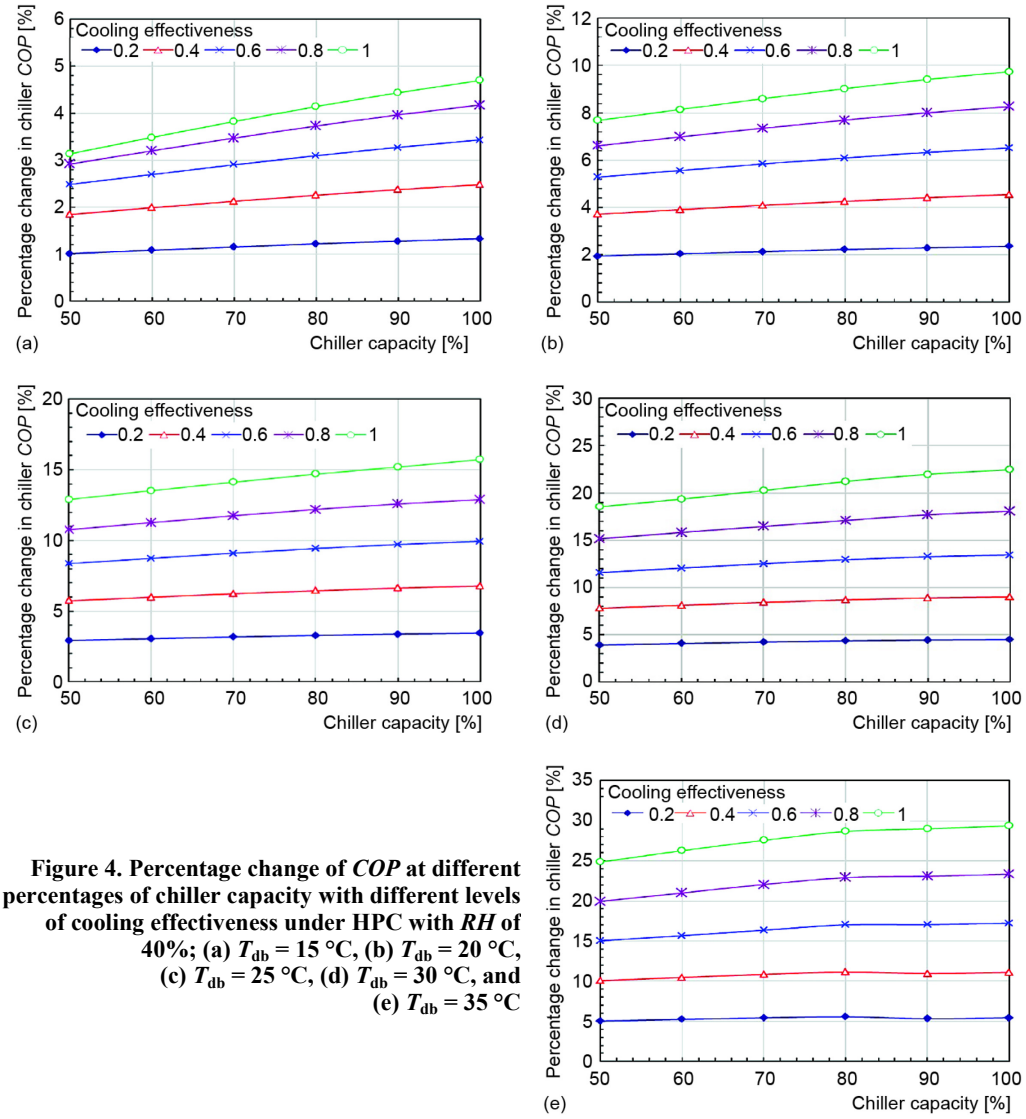

Figure 4. Percentage change of *COP* at different percentages of chiller capacity with different levels of cooling effectiveness under HPC with *RH* of 40%; (a) T_{db} = 15 °C, (b) T_{db} = 20 °C, (c) T_{db} = 25 °C, (d) T_{db} = 30 °C, and (e) T_{db} = 35 °C

chiller capacities under HPC. This is because the heat rejection capacity was enhanced slightly at a low wet bulb depression. The highest percentage increase of *COP* is around 3.5% at an outdoor temperature of 35 °C with a wet bulb depression of 2.5 °C. Under FCTC in fig. 7, the percentage change of *COP* and the chiller capacity have a non-linear relationship at an outdoor temperature of 20 °C or above. A minor *COP* loss may occur when the chiller capacity is below 80% of full capacity and the outdoor temperature is 25 °C or above. The loss is due to the extra power of the mist generation pump and is more significant when the cooling effectiveness drops from 1.

Overall, at a low relative humidity of 40% with a high wet bulb depression, mist precooling enables the chiller *COP* to increase with the chiller capacity. Higher cooling effectiveness would bring a higher percentage increase of chiller *COP*. The increase would be up to

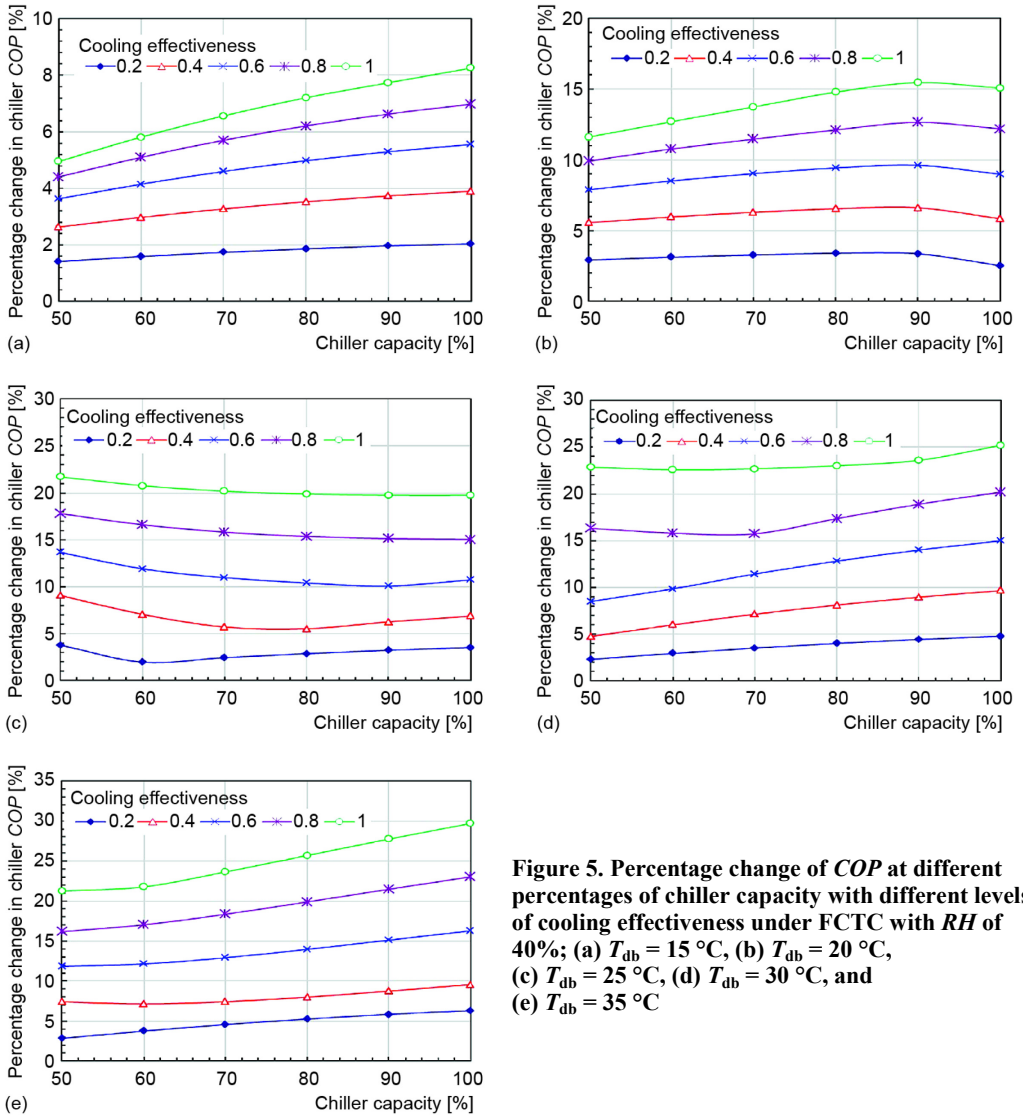

Figure 5. Percentage change of *COP* at different percentages of chiller capacity with different levels of cooling effectiveness under FCTC with *RH* of 40%; (a) T_{db} = 15 °C, (b) T_{db} = 20 °C, (c) T_{db} = 25 °C, (d) T_{db} = 30 °C, and (e) T_{db} = 35 °C

30% under both HPC and FCTC. When the relative humidity increases to 85% with a low wet bulb depression, the percentage increase of chiller *COP* is 3.5% at most. The percentage change of chiller COP has a non-linear relationship with the chiller capacity under FCTC and the cooling effectiveness should be kept as high as possible in order to increase the chiller *COP*. It is expected that the non-linear relationship is associated with the interaction between the reduced outdoor temperature and the control of condenser fans to maintain the condensing temperature at its set point. Experimental work is underway by the authors to examine how nozzles should be placed over the wide condenser area and how their atomization effect is regulated by the orifice size in order to maximize the cooling effectiveness. Variable speed control of condenser fans is found essential to adjust precisely the condensing temperature in response to the reduced outdoor temperature while reducing the fan power at part load operation.

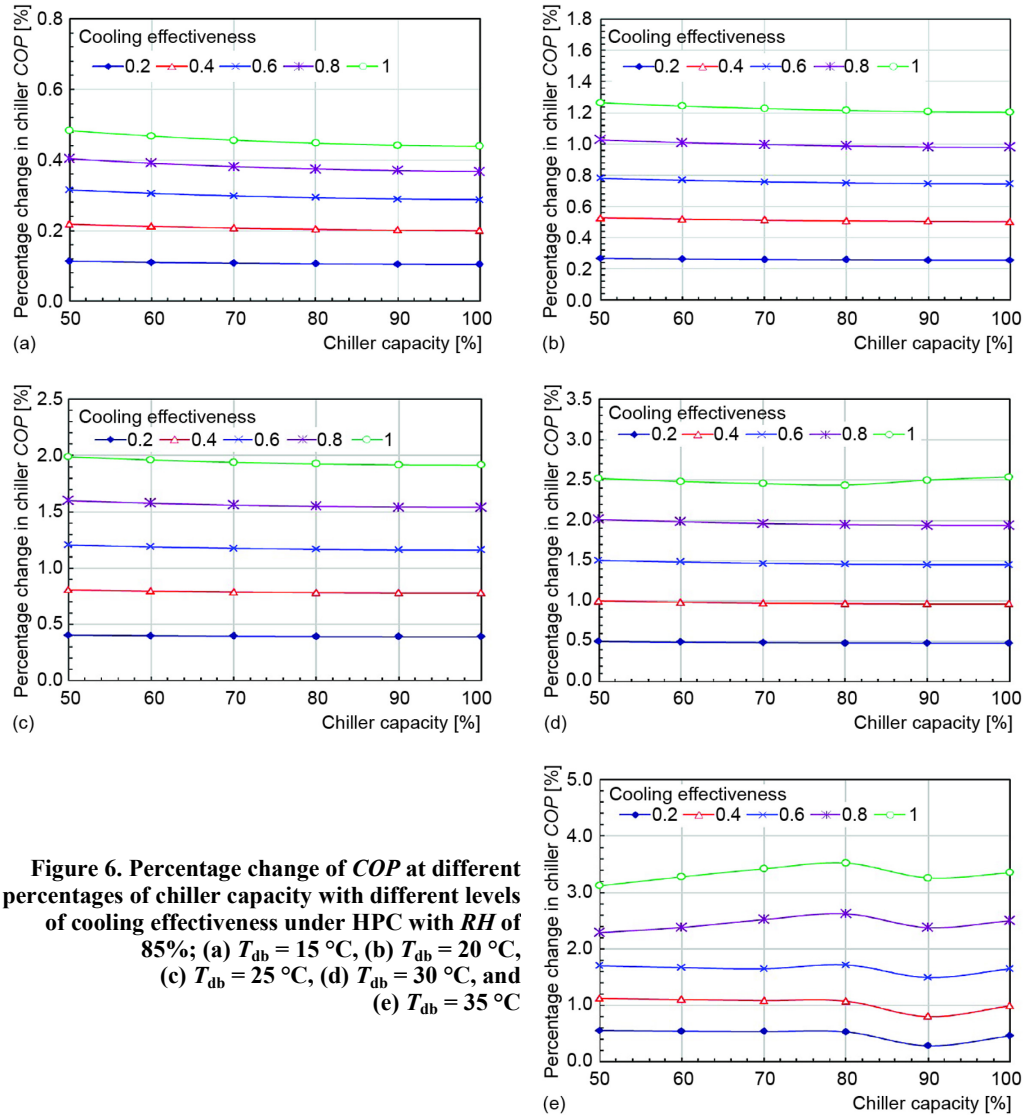

Figure 6. Percentage change of *COP* at different percentages of chiller capacity with different levels of cooling effectiveness under HPC with *RH* of 85%; (a) T_{db} = 15 °C, (b) T_{db} = 20 °C, (c) T_{db} = 25 °C, (d) T_{db} = 30 °C, and (e) T_{db} = 35 °C

Conclusions

This study examines how *COP* of an air-cooled chiller can be enhanced by mist pre-cooling at different levels of cooling effectiveness. The chiller modelled had a rated capacity of 1266 kW with a *COP* of 3.19. Its performance data were used to validate a multivariate regression model, taking into account the variation of condensing temperature under HPC and FCTC and the precooling of outdoor air by a mist generator.

When the relative humidity is 40% with a high wet bulb depression, the *COP* could increase by up to 30% when the chiller operated under HPC or FCTC. The *COP* indeed tends to increase linearly with the chiller capacity, which complements the sequencing control of chillers in a multiple-chiller system. At a high relative humidity of 85% with a small wet

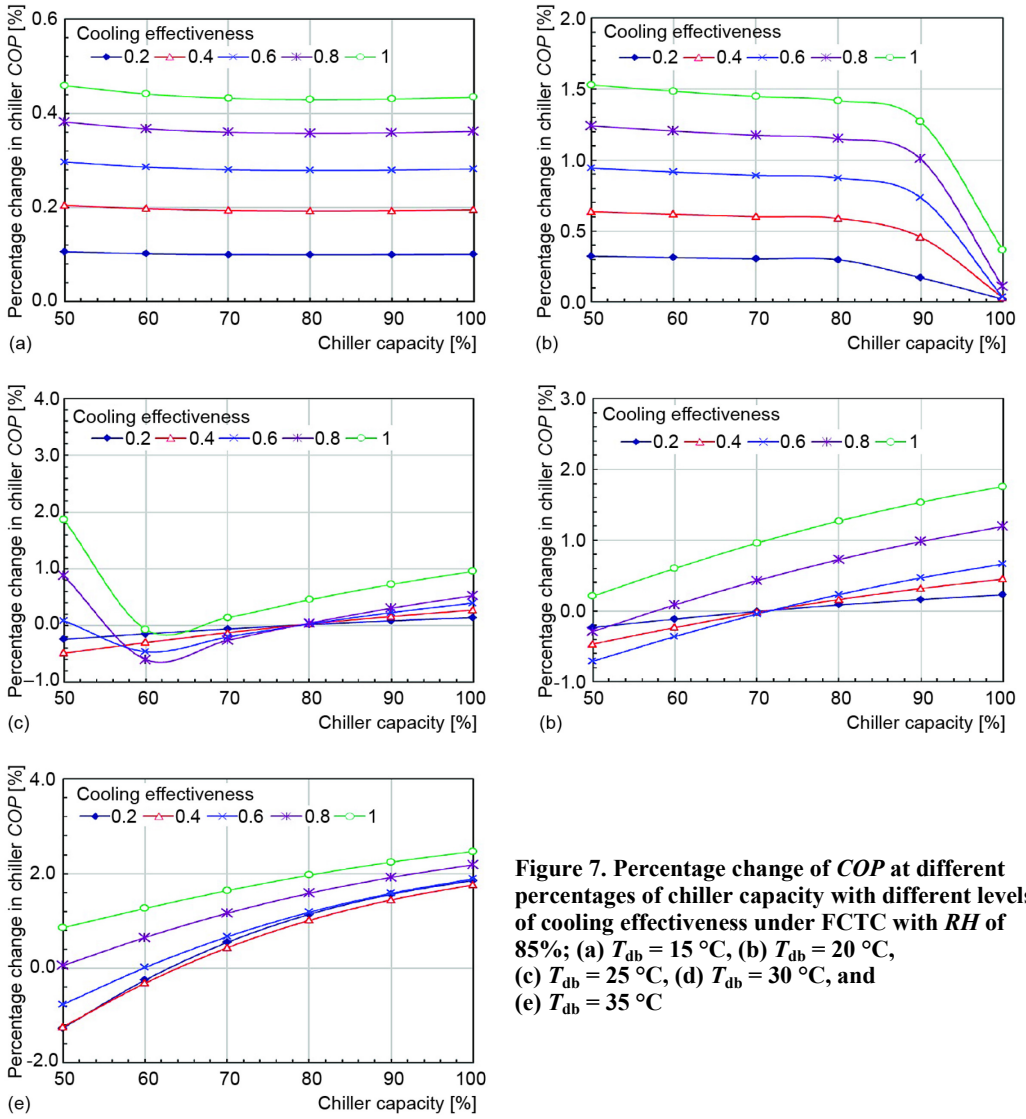

Figure 7. Percentage change of *COP* at different percentages of chiller capacity with different levels of cooling effectiveness under FCTC with *RH* of 85%; (a) T_{db} = 15 °C, (b) T_{db} = 20 °C, (c) T_{db} = 25 °C, (d) T_{db} = 30 °C, and (e) T_{db} = 35 °C

bulb depression, the dynamic control of condensing temperature resulted in a non-linear relationship between the percentage change of *COP* and the cooling effectiveness. It is necessary to maintain the cooling effectiveness as high as possible in order to maximize the *COP*. Further experimental work is required to investigate how the orifice size and layout of nozzles should be used to optimize the atomization effect for maximum cooling effectiveness. The precise adjustment of condensing temperature in response to the reduced condenser air temperature would call for controlling condenser fans at variable speed.

Acknowledgment

This study was supported by a grant from the College of Professional and Continuing Education, an affiliate of The Hong Kong Polytechnic University (Project A/C

4.8C.40.EZ72) and a grant from the Research Grant Council of HKSAR (Project A/C Code: B-Q31R).

Nomenclature

CAPFT – adjusting factor for chiller capacity at full load, [–]
c_p – specific heat capacity, [kJkg^{-1}°C^{-1}]
Eff – heat transfer effectiveness, [-]
EIRFT – adjusting factor for compressor efficiency at full load, [–]
EIRFPLR – adjusting factor for compressor efficiency at part load, [–]
H – specific enthalpy, [kJkg^{-1}]
m – mass flow rate, [kgs^{-1} or Ls^{-1}]
P – electric power, [kW]
PLR – chiller part load ratio, [–]
Q_{cd} – heat rejection, [kW]
Q_{cl} – chiller capacity, [kW]
R^2 – coefficient of determination, [–]
RH – relative humidity, [%]
T – temperature, [°C]
V – air-flow rate, [m^{3}s^{-1}]
W – moisture content, [kgkg^{-1} dry air]

Greek symbols

ρ – density, [kgm^{-3}]
η – cooling effectiveness, [–]

Subscripts

a – condenser air
cc – compressor
cd – condenser
cdae – entering condenser air
cdal – leaving condenser air
ce – mist precooler
cf – condenser fans
chwr – return side of chilled water
chws – supply side of chilled water
db – dry bulb condition of outdoor air
rated – at rated condition
mist – mist
mp – mist generation pump
w – chilled water
wb – wet bulb condition of outdoor air

Superscript:

′ – after mist precooling

References

[1] Wong, N. H., Chong, A. Z. M., Performance Evaluation of Misting Fans in Hot and Humid Climate, *Building and Environment, 45* (2010), 12, pp. 2666-2678
[2] Hamlin, S., *et al*., Enhancing the Performance of Evaporative Spray Cooling in Air Cycle Refrigeration and Air Conditioning Technology, *Applied Thermal Engineering, 18* (1998), 11, pp. 1139-1148
[3] Sawan, R., *et al*., Use of Condensate Drain to Pre-Cool the Inlet Air to the Condensers: A Technique to Improve the Performance of Split Air-Conditioning Units, *HVAC&R Research, 18* (2012), 3, pp. 417-431
[4] Vakiloroaya, V., *et al*., A Review of Different Strategies for HVAC Energy Saving, *Energy Conversion and Management, 77* (2014), Jan., pp. 738-754
[5] Hajidavalloo, E., Eghtedari, H., Performance Improvement of Air-Cooled Refrigeration System by Using Evaporatively Cooled Air Condenser, *International Journal of Refrigeration, 33* (2010), 5, pp. 982-988
[6] Chowdhury, A. A., *et al*., Modelling and Analysis of Air-Cooled Reciprocating Chiller and Demand Energy Savings Using Passive Cooling, *Applied Thermal Engineering, 29* (2009), 8-9, pp. 1825-1830
[7] Rašković, P. O., *et al*., Improving Eco-Sustainable Characteristics and Energy Efficiency of Evaporative Fluid Cooler via Experimental and Numerical Study, *Thermal Science, 12* (2008), 4, pp. 89-103
[8] Hao, X. L., *et al*., Optimizing the Pad Thickness of Evaporative Air-Cooled Chiller for Maximum Energy Saving, *Energy and Buildings, 61* (2013), June, pp. 146-152
[9] Yu, F. W., *et al*., Evaporative Cooling Technologies for Air-Cooled Chillers for Building Energy Performance Improvement, *Advances in Building Energy Research, 10* (2016), 1, pp. 10-19
[10] Yu, F. W., Chan, K. T., Modelling of Improved Energy Performance of Air-Cooled Chillers with Mist Pre-Cooling, *International Journal of Thermal Sciences, 48* (2009), 4, pp. 825-836
[11] ***, U. S. Chiller Services – Energy Solutions, www.uschillerservices.com/energy.html, under Tag: USCS Condenser Air Pre-Cooler
[12] Yang, J., *et al*., Performance Enhancement of Air-Cooled Chillers with Water Mist: Experimental and Analytical Investigation, *Applied Thermal Engineering, 40* (2012), July, pp. 114-120

[13] Yu, F. W., *et al*., Energy Simulation of Sustainable Air-Cooled Chiller System for Commercial Buildings under Climate Change, *Energy and Buildings, 64* (2013), Sept., pp. 162-171
[14] Yu, F. W., Chan, K. T., Simulation and Electricity Savings Estimation of Air-Cooled Centrifugal Chiller System with Mist Pre-Cooling, *Applied Energy, 87* (2010), 4, pp. 1198-1206
[15] Yu, F. W., Chan, K. T., Improved Energy Performance of Air-Cooled Chiller System with Mist Pre-Cooling, *Applied Thermal Engineering, 31* (2011), 4, pp. 537-544
[16] Tissot, J., *et al*., Improved Energy Performance of a Refrigerating Machine Using Water Spray Upstream of the Condenser, *International Journal of Refrigeration, 38* (2014), Feb., pp. 93-105
[17] Tissot, J., *et al*., Air Cooling by Evaporating Droplets in the Upward Flow of a Condenser, *International Journal of Thermal Sciences, 50* (2011), 11, pp. 2122-2131
[18] Liao, Y. D., *et al*., Robustness Analysis of Chiller Sequencing Control, *Energy Conversion and Management, 103* (2015), Oct., pp. 180-190
[19] ***, Air-Conditioning, Heating, and Refrigeration Institute (AHRI), AHRI Standard 550/590-2003-2011 Standard for performance rating of water-chilling packages using the vapor compression cycle, Author press, Arlington, Va, USA
[20] Crawley, D. B., *et al*., EnergyPlus: Creating a New-Generation Building Energy Simulation Program, *Energy and Buildings, 33* (2001), 4, pp. 319-331

Paper submitted: November 12, 2015
Paper revised: March 6, 2016
Paper accepted: March 9, 2016